Cerebral Cortex, July 2020;30: 4140–4157

doi: 10.1093/cercor/bhaa038
Advance Access Publication Date: 28 February 2020
Original Article

ORIGINAL ARTICLE

A Lifespan fMRI Study of Neurodevelopment Associated with Reading Chinese

Wai Ting Siok[1,†], Fanlu Jia[2,3,†], Chun Yin Liu[1], Charles A. Perfetti[4] and Li Hai Tan[3]

[1]Department of Linguistics, The University of Hong Kong, Hong Kong, [2]School of Education and Psychology, University of Jinan, Jinan 250022, China, [3]Center for Language and Brain, Shenzhen Institute of Neuroscience, Shenzhen 518060, China and [4]Learning Research and Development Center, University of Pittsburgh, Pittsburgh, PA 15260, USA

Address correspondence to Wai Ting Siok, Department of Linguistics, The University of Hong Kong, Pokfulam Road, Hong Kong. Email: siok@hku.hk; Li Hai Tan, Center for Language and Brain, Shenzhen Institute of Neuroscience, Shenzhen 518060, China. Email: tanlh@sions.cn.
[†]Wai Ting Siok and Fanlu Jia have contributed equally to this work.

Abstract

We used functional magnetic resonance imaging (fMRI) to map the neural systems involved in reading Chinese in 125 participants 6–74 years old to examine two theoretical issues: how brain structure and function are related in the context of the lifetime neural development of human cognition and whether the neural network for reading is universal or different across languages. Our findings showed that a common network of left frontal and occipital regions typically involved in reading Chinese was recruited across all participants. Crucially, activation in left mid-inferior frontal regions, fusiform and striate–extrastriate sites, premotor cortex, right inferior frontal gyrus, bilateral insula, and supplementary motor area all showed linearly decreasing changes with age. These findings differ from previous findings on alphabetic reading development and suggest that early readers at age 6–7 are already using the same cortical network to process printed words as adults, though the connections among these regions are modulated by reading proficiency, and cortical regions for reading are tuned by experience toward reduced and more focused activation. This fMRI study has demonstrated, for the first time, the neurodevelopment of reading across the lifespan and suggests that learning experience, instead of pre-existing brain structures, determines reading acquisition.

Key words: Chinese reading, functional and structural development, lifespan brain development, neural development of reading, reading development

Introduction

Research examining how cortical specialization emerges during development has been proliferative (Bock et al. 2011; Briggman et al. 2011), yet few studies have explored the development of the cortical system across the lifespan. This study investigated the neural development of logographic Chinese reading across the lifespan, from childhood (age 6) to late adulthood (age 74), scrutinizing two theoretical issues. First, we examine how brain structure and function are related in the context of the lifetime neural development of human cognition. Three hypotheses have been proposed. The "structure-based account" holds that the emergence of a skill is contingent upon the onset of the functioning and maturation of brain regions specialized for that skill (Johnson 2001) and that structural fingerprints determine

functional fingerprints (Carreiras et al. 2009; Saygin et al. 2012, 2016; Srihasam et al. 2014; Osher et al. 2016). It is well known that gray matter (GM) volumes increase before puberty and then decline until old age while white matter (WM) volumes increase linearly from early childhood to adolescence, and after that, they increase at a slower rate until reaching a plateau by the fourth decade of life (Giedd et al. 1999; Courchesne et al. 2000; Gogtay et al. 2004; Pfefferbaum et al. 2013; Tamnes et al. 2017). Therefore, the developmental patterns of both GM and WM show an inverted U-shaped curve across the lifespan. Cortical activations may show the same patterns as anatomical changes across the human lifespan. The "experience-based account" assumes that the stereotyped locations develop due to the specific tuning of neurons in a cortical region to shape features and the cognitive functions subserved by a brain region are determined by the amount and type of information it receives and transmits during development (Bedny 2017). In this account, regional cortical activation is a function of the level of skill (Srihasam et al. 2014). The "interactive specialization account" argues that cognitive functions are supported by multiple specialized cortical regions that are highly interactive and dynamic in nature (Friston and Price 2001). The neural development of cognitive skills, thus, should involve changes in connections among those specialized regions (Johnson 2001). To date, these hypotheses have not been tested in terms of the lifespan development of cognitive skills.

Second, we explore whether the neural network for reading is universal or different across languages. The neuronal recycling hypothesis (Dehaene 2009) postulates that the successful acquisition of evolutionarily recent reading skills, which takes years and explicit effort to achieve full potency, is contingent upon the encroachment and fine-tuning of pre-existing, genetically evolved ventral visual cortical areas to process the novel visual stimuli and to integrate the visual outputs with phonology and meaning. A key issue under debate is whether print–sound mapping engages a universal or culturally diverse pathway across languages (Dehaene 2009; Coltheart 2014). The universal reading perspective assumes that because all writing systems encode spoken languages that are subserved by a universal neural network and that share universal visual features, an identical brain network should be used for all languages regardless of the level of reading proficiency (Dehaene and Cohen 2011; Nakamura et al. 2012; Rueckl et al. 2015). In contrast, the property-based perspective argues that no universal visual features could be identified for all writing systems; thus, different cortical regions must be recruited to support specific visual features (Coltheart 2014). Thus, differential neuronal networks may be observed at the beginning of reading development across different languages; even if beginner readers of a writing system initially use the same neural system that was originally used for speech processing to process the visual mode of the language, brain regions that support the computation of features unique to the writing system will be co-opted, gradually leading to the development of cultural-specific reading systems.

Using functional magnetic resonance imaging (fMRI), we attempted to discover brain activity patterns during a reading task in 125 native Chinese speakers across a long age span (60 children aged 6–11 and 65 adults aged 18–74). We devised a phonology-based reading task because reading development is closely associated with phonological processing in all languages (Goswami and Ziegler 2006; Carreiras et al. 2009) and because different writing systems differ principally in print–sound mappings. In the experimental task, participants judged whether two simultaneously presented words had the same pronunciation. In the control task, participants made font size judgments, deciding whether two visually presented words had the same physical size.

Materials and Methods

Participants

One hundred thirty native Chinese participants in Beijing participated in the fMRI experiments. Data from four children with behavioral performance below chance level (58%) and from one adult with excessive head motion during scanning were excluded from the analysis. The final sample consisted of 125 participants, including 28 beginner readers who had been reading for less than 4 months (17 males and 11 females, mean age = 7 years 4 months, standard deviation [SD] = 3.3 m), 32 intermediate readers (20 males and 12 females, mean age = 10 years 3 months, SD = 5.4 months), 34 younger adult readers (17 males and 17 females, mean age = 25 years 0 month, SD = 55.3 month), and 31 older adult readers (19 males and 12 females, mean age = 50 years 8 months, SD = 119.3 months). Participants were paid for their participation and gave informed consent according to guidelines set by the Administrative Panels on Human Participants in Medical Research of the Beijing MRI Center for Brain Research at the Chinese Academy of Sciences and the University of Hong Kong. All participants had no history of language disorders or neurological illness. Participants were strongly right-handed, as judged by the handedness inventory devised by Snyder and Harris (1993). A detailed demographic information of the participants is presented in Table 1.

Stimuli and Experimental Design

The functional activation task used in this study was a homophone judgment task (to judge whether two synchronously presented Chinese characters had identical pronunciation). In the control condition, participants decided whether a pair of characters had the same physical size (font size decision). All Chinese characters used were commonly encountered and selected from grade 1 Chinese language textbooks to ensure that younger readers could also complete the tasks. The visual complexity of the characters was matched across all conditions.

A blocked design was used, in which six blocks of font size judgments (the baseline task) were alternated with six blocks of homophone judgments (the experimental task). Each block consisted of a 2-s instruction and 8 trials. In each trial, a pair of characters was synchronously presented for 1500 ms, one above and one below a fixation cross, followed by a 1500-ms blank interval. Participants indicated a positive response by pressing the key corresponding to the index finger of their right (dominant) hand and a negative response by pressing the key corresponding to the index finger of their left (nondominant) hand. They were asked to perform the tasks as quickly and accurately as possible.

Participants' reading ability was evaluated by asking them to read aloud 400 Chinese characters (the character reading task). These characters were selected from textbooks used in primary schools in Beijing for first to sixth graders, with 40 characters being selected from each grade level. The remaining 160 characters were selected from low-frequency characters in a linguistic corpus that was not covered in primary school

Table 1 Demographic information and in-scanner behavioral performance of participants

		(1) Beginning readers	(2) Intermediate readers	(3) Younger adults	(4) Older adults	One-way ANOVA *P* value
Number of participants		28	32	34	31	
Mean age		7 years 4 months (3.3 months)	10 years 3 months (5.4 months)	25 years 0 months (55.3 months)	50 years 8 months (119 months)	
Gender		17M 11F	20M 12F	17M 17F	19M 12F	
Raven (in percentile)		81 (17)	76 (7)	N/A	N/A	
Chinese reading score (total score = 400)		69 (21)	200 (25)	310 (71.8)	186 (61.6)	<0.001; (1) < (2) = (4) < (3)
Experimental task	**Accuracy (%)**	75 (9.7)	82 (10.9)	95 (3.8)	95 (5.1)	<0.001; (1) < (2) < (3) = (4)
Baseline task	**Accuracy (%)**	83 (9.4)	88 (8.6)	94 (5.0)	95 (4.5)	<0.001; (1) < (2) < (3) = (4)

		Children	**Adults**	**Children versus adults *P* value**
		All subjects		
Number of participants		60	65	
Mean age		8 years 11 months (18 months)	37 years 3 months (180 months)	
Age range		6 years 9 months–11 years 5 months	18 years 7 months–74 years 3 months	
Gender		37M 23F	36M 29F	
Raven (in percentile)		81 (17)	N/A	
Chinese reading score		139 (70)	245 (90)	<0.005
Experimental task	**Accuracy (%)**	79 (10.7)	95 (4.8)	<0.001
Baseline task	**Accuracy (%)**	85 (9.9)	95 (4.4)	<0.001
		Character reading and homophone decision accuracy matched		
Number of participants		24	24	
Mean age		9 years 11 months (14 months)	39 years 7 months (194 months)	
Age range		7 years 3 months–11 years 5 months	19 years 8 months–74 years 3 months	
Gender		13M 11F	15M 9F	
Chinese reading score		186 (47)	214 (101)	= 0.22
Experimental task	**Accuracy (%)**	88 (5.1)	90 (4.1)	= 0.25
Baseline task	**Accuracy (%)**	92 (3.8)	94 (5.1)	= 0.10

SDs in parentheses.

textbooks. Characters were arranged by increasing difficulty (as determined by grade level and visual complexity or stroke number). Participants were asked to read the characters aloud as quickly and accurately as possible within 3 min. The test was discontinued when a participant made 10 consecutive errors. Six adults did not return for the reading test; thus, only 59 adults were tested on their reading ability. The average reading scores of children and adults were 139 (SD = 70) and 245 (SD = 90), respectively.

Image Acquisition

Whole-brain imaging data were acquired on a 3-T Siemens MRI scanner at the Beijing MRI Center for Brain Research of the Chinese Academy of Sciences using a T_2*-weighted gradient-echo echo-planar imaging (EPI) sequence (TE = 30 ms, TR = 2 s, flip angle = 90°, slice thickness = 4 mm, field of view = 22 cm). Thirty-two contiguous axial slices were acquired parallel to the AC–PC line. Visual stimuli were presented via a liquid crystal display projector and back-projected onto a projection screen placed at the end of the scanner bore. Participants viewed the rear projection screen through a mirror attached to the head coil. Each functional scan was preceded by 6 s of dummy scans to allow for T_1 equilibration. At the end of each imaging run, participants viewed a fixation cross continuously for 60 s. High-resolution ($1 \times 1 \times 1$ mm^3) anatomical images were acquired using a T_1-weighted, 3D gradient-echo sequence.

Data Analysis

Functional Data

The functional data were preprocessed and analyzed with SPM8 (Wellcome Department of Cognitive Neurology, University College London, London) using MATLAB 7.5.0 (MathWorks). The first three volumes of each fMRI scan were discarded to allow for T_1 equilibration, and the remaining volumes of each subject's data set were realigned to the first volume of the functional run and resliced to correct artifacts due to head movements. Volumes were then spatially normalized to an EPI template based on the ICBM152 stereotactic space, an approximation of canonical space (Talairach and Tournoux 1988), and were resampled into $2 \times 2 \times 2$ mm cubic voxels. This normalization procedure has been shown to be appropriate for children aged 7 and above (Burgund et al. 2002) and would allow comparisons of activations across participants of different ages. The images were spatially smoothed by an isotropic Gaussian kernel (6-mm full width at half-maximum).

All functional images were inspected for artifacts using the artifact detection toolbox (http://www.nitrc.org/projects/artifact_detect). An outlier was defined if an image exceeded 3 SDs from the mean global signal or if between-image head movement exceeded a prespecified threshold (0.5 mm for translation or 0.02 radians for rotation). Each outlier image was modeled as a single regressor of no interest and was excluded in the first-level statistical analysis. On average, 1.1% (SD = 1.9%) and 1.2% (SD = 1.4%) of the images in the homophone scan were defined as outliers in children and adults, respectively, and the mean translational movement (x, y, z) for children and adults was 0.080 (SD = 0.037) and 0.205 (SD = 0.213), respectively. Independent-samples t-tests revealed that the two groups did not differ significantly in the number of outlier images [$t(123) = 0.19$, $P = 0.85$], but the head movement of adults was significantly larger than that of children [$t(123) = 4.496$, $P < 0.001$]. As age and mean translational movement were positively correlated ($r = 0.61$, $P < 0.001$), the six motion parameters obtained during image realignment were included in the first-level model as additional regressors of no interest to minimize motion artifacts across ages. An individual subject's activation t-map was generated using a general linear model (Friston et al. 1995), in which time series were convolved with the canonical hemodynamic response function.

The data were globally scaled, high-pass filtered at 128 s, and corrected for serial correlations using a first-order autoregressive AR(1) model. The contrast images between experimental and baseline conditions from each subject were taken into a second-level random effects model for group analysis. Whole-brain activation maps averaged across all participants were computed for homophone > font size judgment by using one-sample t-tests. To evaluate age differences in brain activation, we contrasted brain activity between children and adults using an independent-samples t-test ($P < 0.05$ FDR corrected at the voxel level and $P < 0.05$ FWE corrected at the cluster level) and conducted whole-brain regression analyses with age as a continuous predictor variable ($P < 0.05$ FDR corrected at the voxel level and $P < 0.05$ FWE correction at the cluster level). In addition, activation clusters in the all-participant homophone > font activation map that survived the voxel-level $P < 0.001$ FWE threshold were defined as regions of interest (ROIs) for the homophone condition. Pearson's r correlation coefficients (two-tailed) between average BOLD contrast estimates within these ROIs and behavioral measures (age and character reading performance) were computed across participants using SPSS 23.0. Brain regions are estimated from Talairach and Tournoux (1988) after adjustments for differences between the MNI and Talairach coordinates (http://www.talairach.org/).

To further investigate how brain regions convey information between one another, effective connectivity in four regions (see Results) associated with Chinese reading was computed by dynamic causal modeling (DCM). DCM models neuronal activity by estimating parameters that represent 1) the intrinsic connections between regions, 2) the modulatory effects of experimental tasks on the changes in the coupling between regions, and 3) the direct effects of experimental inputs on particular brain regions (Friston et al. 2003). In a DCM analysis, models or families of models that represent brain region connections are first specified, and the models/families are then evaluated against the empirical data by a process called Bayesian model selection (BMS), in which the complexity and accuracy of the models/families are taken into account (Penny et al. 2004). All analyses were performed using SPM 12 (https://www.fil.ion.ucl.ac.uk/spm/software/spm12/).

Anatomical Data

All anatomical images were processed and analyzed using the Computational Anatomy Toolbox (CAT12; http://www.neuro.uni-jena.de/cat/) implemented in SPM12 using a standard protocol (http://www.neuro.uni-jena.de/cat12/CAT12-Manual.pdf). Voxel-based morphometry analysis was conducted to estimate the GM and WM density of participants using a fully automated algorithm, and each participant's modulated and normalized GM and WM tissue segments were smoothed using a 12-mm FWHM Gaussian kernel. Pearson's r correlation coefficients (two-tailed) between gray and WM density within these ROIs and age were computed across participants.

Results

Demographic information and behavioral performance for all participants are presented in Table 1. The mean character reading performance (out of 400) was 69, 200, 310, and 186, and the in-scanner behavioral performance (percentage correct) on homophone decision was 75, 82, 95, and 95 for beginner readers, intermediate readers, younger adult readers, and older adult readers, respectively. Character reading performance and homophone decision score were moderately correlated ($r = 0.55$, $P < 0.001$). Thus, the homophone decision task could be considered a good measurement of reading abilities.

Consistent with previous findings (Siok et al. 2004; Tan et al. 2005; Xue et al. 2005; Gabrieli 2009; Wu et al. 2012), we found reading Chinese, as indexed by orthography-to-phonology mapping in our task, is subserved by a brain network that includes the left mid-inferior frontal regions (BAs 9/44/45/47), left precentral gyrus (BA 6), right inferior frontal gyrus (BA 47), superior medial frontal regions (BAs 6/8), dorsal anterior cingulate gyrus (BA 32), insula, left superior parietal lobule (SPL) (BA 7), left striate cortex (BA 17), bilateral extrastriate cortices (BAs 18/19), left fusiform gyrus (BA 37), caudate nucleus, putamen, thalamus, and cerebellum (Fig. 1 and Table 2). For each of the four age groups, similar brain networks were observed, with younger readers generally showing activation that was more bilateral and more extensive (more voxels) within these regions than older readers (c.f. Turkeltaub et al. 2003). Because brain activity differences between the two child groups and between the two adult groups were not significant (at $P < 0.001$ uncorrected), we collapsed the two child groups and the two adult groups in the subsequent group comparison analyses.

We performed whole-brain regression analysis with age as a predictor variable to find out which brain regions showed activity that varied with age, with voxel-level threshold at $P < 0.05$ FDR corrected and cluster-level threshold at $P < 0.05$ FWE corrected (Fig. 2A). We found significant negative correlations at bilateral insula (left, $x = -36$, $y = 11$, $z = -6$, $r = -0.46$, $P < 0.001$; right, $x = 32$, $y = 13$, $z = -6$, $r = -0.50$, $P < 0.001$), right mid-superior frontal gyrus (BA 10, $x = 24$, $y = 51$, $z = 18$, $r = -0.40$, $P < 0.001$), dorsal anterior cingulate cortex (BA 32, $x = 10$, $y = 30$, $z = 24$, $r = -0.46$, $P < 0.001$), right extrastriate cortex (BA 19, $x = 53$, $y = -63$, $z = 16$, $r = -0.40$, $P < 0.001$), and bilateral thalamus (left, $x = -8$, $y = -24$, $z = 16$, $r = -0.49$, $P < 0.001$; right, $x = 8$, $y = -13$, $z = 4$, $r = -0.45$, $P < 0.001$) (Fig. 2B). No positive correlation was seen. Within these seven regions, BOLD activation correlated mildly with character reading at all except the right thalamus

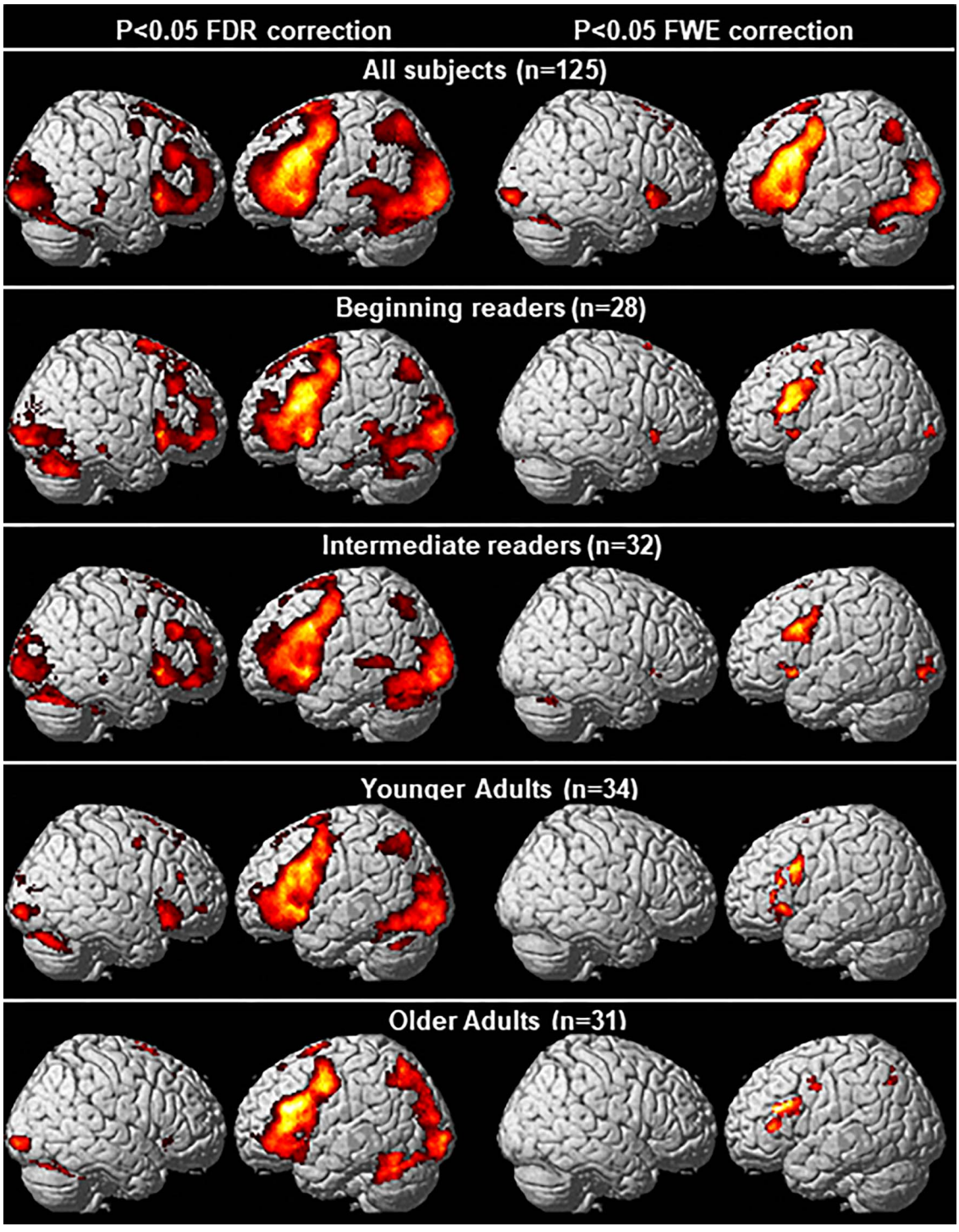

Figure 1. Brain regions showing significant activation during homophone judgment. Results from two voxel-level thresholds are shown: $P < 0.05$ FDR correction (left panels) and $P < 0.05$ FWE correction (right panels). Cluster-level threshold was set at $P < 0.05$ FWE correction for both of them.

regions (left insula, $r = -0.28$, $P < 0.005$; right insula, $r = -0.25$, $P < 0.01$; cingulate, $r = -0.26$, $P < 0.005$; right mid-superior frontal gyrus, $r = -0.19$, $P < 0.05$; right extrastriate, $r = -0.23$, $P < 0.05$; left thalamus, $r = -0.21$, $P < 0.05$); moderately with GM density at bilateral insula (left, $r = 0.39$, $P < 0.001$; right, $r = 0.36$, $P < 0.001$), cingulate ($r = 0.42$, $P < 0.001$), and right mid-superior frontal gyrus ($r = 0.33$, $P < 0.001$); and mildly with WM density at right insula ($r = -0.27$, $P < 0.005$) and right extrastriate cortex ($r = -0.21$, $P < 0.05$).

To examine specific regions that exhibited developmental changes in the reading network, we followed previous studies investigating the neurodevelopment of memory and used the ROIs approach (Golarai et al. 2007; Ofen et al. 2007). We identified activation clusters in the all-participant homophone > font

Table 2 Coordinates of activation peaks during homophone > font size judgment in (A) all participants, (B) children, and (C) adults

			Talairach coordinates				
	mm^3	BA	x	y	z	Peak t	Peak Z
A. Across all participants ($n = 125$, voxel-level threshold at $P < 0.001$ FWE correction)							
Left mid-inferior frontal cortex	6089	44	−44	17	25	17.64	Inf
	″	45	−48	31	4	13.00	Inf
	″	9	−48	4	42	12.38	Inf
	″	47	−32	21	−1	12.35	Inf
	″	44	−53	14	11	10.54	Inf
	″	47	−48	42	−5	9.41	Inf
Left precentral gyrus	″	6	−36	0	44	10.06	Inf
Right inferior frontal cortex/insula	674	47	32	25	−5	12.16	Inf
Medial frontal cortex and the SMA	2592	8	−2	20	47	14.70	Inf
	″	6	−4	12	53	14.46	Inf
Cingulate gyrus	″	32	8	29	26	8.68	7.65
Left SPL	568	7	−28	−62	45	11.43	Inf
Left striate cortex	6515	17	−10	−85	4	11.51	Inf
	″	17	−22	−95	3	11.42	Inf
	″	17	−8	−75	13	9.59	Inf
	″	17	−17	−75	11	9.48	Inf
Left extrastriate cortex	″	18	−30	−89	−1	10.99	Inf
	″	19	−24	−66	−3	9.56	Inf
	″	19	−36	−83	6	9.47	Inf
	″	19	−28	−77	19	9.39	Inf
Right extrastriate cortex	″	18	28	−93	1	9.75	Inf
Left fusiform gyrus	″	37	−50	−55	−12	9.36	Inf
		37	−46	−59	−24	8.54	7.56
Right cerebellum	″		10	−77	−16	13.70	Inf
	″		32	−63	−20	11.19	Inf
	″		32	−59	−22	11.00	Inf
	″		36	−69	−18	9.47	Inf
	″		22	−69	−18	9.39	Inf
Putamen	463		12	2	2	8.75	7.71
Caudate nucleus	″		20	−3	22	8.95	7.83
	″		12	8	11	8.91	7.81
	1313		−16	−1	18	12.84	Inf
	″		−14	6	7	12.57	Inf
Thalamus	″		−4	−9	10	7.69	6.94
B. Children ($n = 60$, voxel-level threshold at $P < 0.05$ FWE correction)							
Medial frontal cortex	2750	8	−2	20	49	15.75	Inf
	″	8	−2	30	46	11.50	Inf
Cingulate gyrus	″	32	10	23	38	10.55	Inf
	″	32	−8	23	32	9.10	7.20
	″	32	8	29	26	9.10	7.10
	″	24	12	32	13	5.60	5.00
SMA	″	6	−4	3	62	9.70	7.50
Left mid-inferior frontal cortex	5134	44	−44	19	25	14.50	Inf
	″	9/44	−50	15	29	13.38	Inf
	″	44	−44	7	31	12.34	Inf
	″	6	−38	1	50	8.85	7.03
	″	46	−48	39	5	8.61	6.90
	″	11	−46	40	−12	6.33	5.51
Left inferior frontal cortex/insula	″	47	−38	17	−3	11.95	Inf
	″	47	−30	21	1	10.47	7.83
Left inferior frontal cortex	″	45	−53	26	17	10.08	7.65
	″	45	−50	29	4	8.87	7.04
Left precentral gyrus	″	6	−48	0	46	10.21	7.71
Right insula	830		32	23	−1	12.21	Inf
Left extrastriate cortex	2468	18	−32	−87	1	10.11	7.67
	″	18	−28	−95	3	9.82	7.53
Left striate cortex	″	17	−10	−85	4	8.27	6.71
Right extrastriate cortex	156	18	30	−91	1	7.99	6.55

(Continued)

Table 2 Continued

			Talairach coordinates				
	mm^3	BA	x	y	z	Peak t	Peak Z
	″	18	36	−86	−2	7.69	6.37
	″	18	24	−99	3	7.28	6.12
	299	18	16	−79	19	7.55	6.29
Right cuneus	″	17	10	−87	8	7.24	6.10
	″	17	16	−73	13	6.78	5.80
C. Adults ($n = 65$, voxel-level threshold at $P < 0.05$ FWE correction)							
Left mid-inferior frontal cortex	3613	44	−46	17	25	11.54	Inf
	″	45	−48	31	4	11.51	Inf
	″	45/46	−46	26	17	10.39	Inf
	″	45	−46	15	20	9.84	7.65
	″	9	−38	2	37	8.68	7.03
	″	44	−50	12	12	8.54	6.95
	″	9	−48	4	42	8.42	6.88
	″	47	−44	31	−7	7.01	6.01
	″	6	−26	0	46	6.42	5.62
	″	10	−42	41	−2	6.31	5.54
SMA	954	6	−4	11	55	9.31	7.37
	″	6	−4	9	62	9.25	7.34
Medial frontal cortex	″	6	−4	18	45	8.21	6.76
Right inferior frontal cortex	121	47	32	25	−5	7.27	6.18
Left striate cortex	1904	17	−10	−85	6	8.85	7.13
		17	−10	−77	17	7.90	6.58
	″	17	−14	−71	13	7.68	6.44
Left extrastriate cortex	203	18	−28	−75	22	8.42	6.88
	″	19	−36	−81	17	5.89	5.24
	″	19	−28	−86	19	5.54	4.99
	280	18	−22	−95	3	7.53	6.35
	″	18	−30	−91	−2	7.28	6.19
	″	19	−38	−81	6	6.20	5.46
Left fusiform gyrus	55	37	−53	−59	−12	7.09	6.07
	″	37	−51	−49	−13	5.60	5.04
Right extrastriate cortex	85	18	22	−93	0	6.93	5.97
Caudate nucleus	216		−16	−3	19	6.97	5.99
	″		−14	6	5	6.31	5.55
	″		−16	−12	23	5.57	5.01
Right cerebellum	422		14	−75	−16	9.06	7.24
	″		26	−63	−19	7.02	6.02
	″		34	−65	−20	6.32	5.55

activation map that survived the stringent voxel-level $P < 0.001$ FWE threshold as ROIs. Seven ROIs were identified (Fig. 3, Table 3), including the left mid-inferior frontal regions (ROI 1), medial frontal cortex and supplementary motor area (SMA) (ROI 2), left fusiform gyrus (FG) and striate–extrastriate cortices (ROI 3), left caudate nucleus and thalamus (ROI 4), right inferior frontal cortex and insula (ROI 5), left SPL (ROI 6), and right caudate nucleus and putamen (ROI 7).

Within the seven ROIs, Pearson's r correlation coefficients between (a) age and BOLD signal activation, (b) age and activation cluster size, (c) age and GM density, (d) age and WM density, (e) GM density and BOLD signal activation, (f) WM density and BOLD signal activation, (g) character reading and BOLD signal activation, (h) character reading and activation cluster size, (i) character reading and GM density, and (j) character reading and WM density were computed across participants (Fig. 3, Table 3), and independent-samples t-tests between the two age groups were computed for four brain measures: (a) BOLD signal activation, (b) activation cluster size, (c) GM density, and (d) WM density (Fig. 4, Table 4). BOLD signal activation at six of these functionally defined ROIs showed significant negative correlations with age as well as character reading and was significantly different between children and adults (two-tailed, Holm–Bonferroni corrected at $P < 0.05$). These ROIs included the left mid-inferior frontal regions [ROI 1, $r = -0.33$, $P < 0.001$ for age and $r = -0.23$, $P < 0.05$ for character reading; $t(123) = 3.96$, $P < 0.001$], medial frontal cortex and SMA [ROI 2, $r = -0.38$, $P < 0.001$; $t(123) = 5.37$, $P < 0.001$ for age and $r = -0.33$, $P < 0.001$ for character reading], left FG and striate–extrastriate cortices [ROI 3: $r = -0.24$, $P < 0.01$; $t(123) = 2.51$, $P < 0.05$ for age and $r = -0.19$, $P < 0.05$ for character reading], left caudate nucleus and thalamus [ROI 4, $r = -0.33$, $P < 0.001$; $t(123) = 4.90$, $P < 0.001$ for age and $r = -0.32$, $P < 0.001$ for character reading], right inferior frontal cortex and insula [ROI 5: $r = -0.43$, $P < 0.001$; $t(123) = 5.25$, $P < 0.001$ for age and $r = -0.22$, $P < 0.05$ for character reading], and right caudate nucleus and putamen [ROI 7, $r = -0.25$, $P < 0.01$; $t(123) = 3.60$, $P < 0.001$ for age and $r = -0.20$, $P < 0.05$ for character reading]. BOLD activity at the left SPL (ROI 6) did not vary with

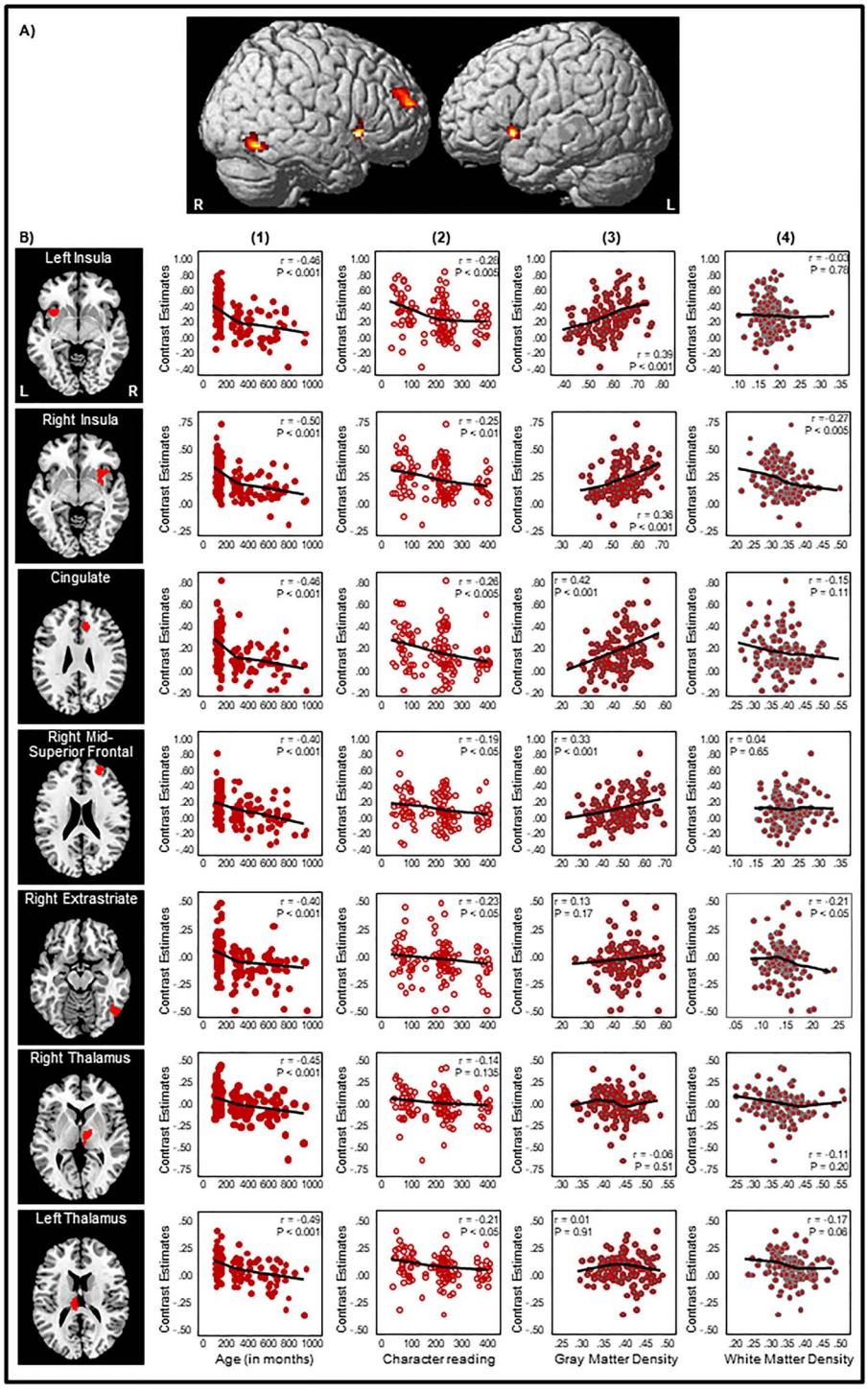

Figure 2. (*A*) Negative correlations from the whole-brain regression analysis with age as a predictor variable. Voxel-level threshold was set at $P < 0.05$ FDR corrected, cluster-level threshold at $P < 0.05$ FWE corrected. (*B*) Correlation plots at the left insula ($x = -36$, $y = 11$, $z = -6$), right insula ($x = 32$, $y = 13$, $z = -6$), dorsal anterior cingulate gyrus (BA 32, $x = 10$, $y = 30$, $z = 24$), right mid-superior frontal gyrus (BA 10, $x = 24$, $y = 51$, $z = 18$), right extrastriate cortex (BA 19, $x = 53$, $y = -63$, $z = 16$), right thalamus ($x = 8$, $y = -13$, $z = 4$), and left thalamus ($x = -8$, $y = -24$, $z = 16$) between BOLD contrast estimates and (1) age, (2) character reading, (3) GM density, and (4) WM density in the second to fifth columns. In each scatterplot, a fit line was added by using a local regression (LOESS) method (Epanechnikov kernel, 80% of points to fit, 95% confidence intervals).

age [$r = 0.02$, $P = 0.86$; $t(123) = 0.04$, $P = 0.97$] or character reading ($r = -0.12$, $P = 0.21$).

Average activation cluster size showed significant negative correlations with age and was significantly different between children and adults in the medial frontal cortex and SMA [ROI 2, $r = -0.25$, $P < 0.01$; $t(123) = 4.36$, $P < 0.001$] and right inferior frontal cortex and insula [ROI 5, $r = -0.22$, $P < 0.05$; $t(123) = 3.53$, $P < 0.01$]. The activation size at the left caudate nucleus and thalamus

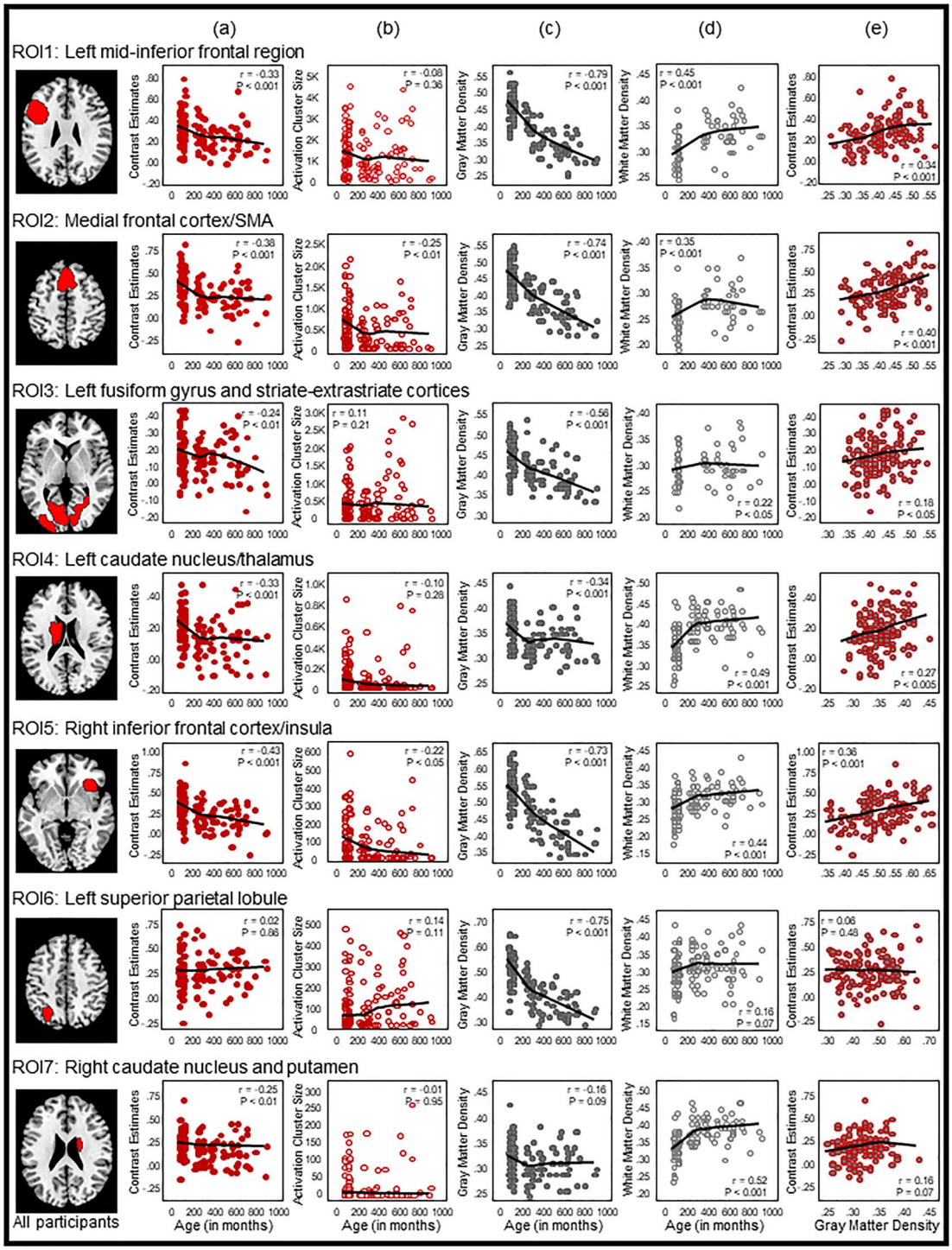

Figure 3. ROI-based Pearson correlation analyses. Seven ROIs surviving the stringent voxel-level $P < 0.001$ FWE threshold in the all-participant homophone > font activation map were selected. Pearson correlations between age and (*a*) BOLD signal activity, (*b*) activation cluster size, (c) GM density, and (*d*) WM density at each of the seven ROIs are shown in columns (*a*)–(*d*), respectively. Columns (*e*) and (*f*) respectively show Pearson correlations of BOLD signal activity with GM density and WM density. Pearson correlations between Chinese character reading performance and BOLD signal activity, activation cluster size, GM density and WM are shown, respectively, in columns (*h*) to (*j*). In each scatterplot, a fit line was added by using a local regression (LOESS) method (Epanechnikov kernel, 80% of points to fit, 95% confidence intervals).

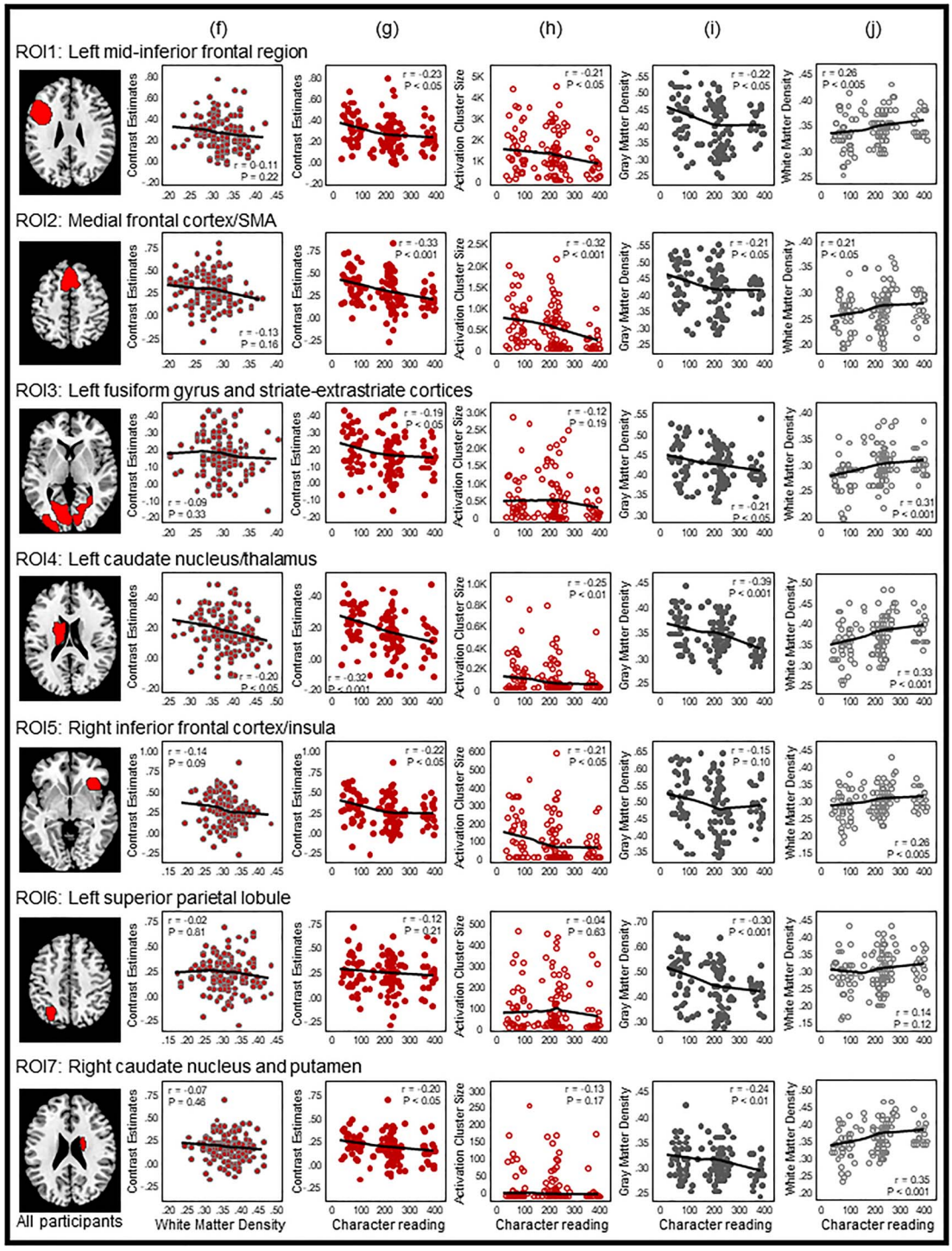

Figure 3. Continued.

(ROI 4) showed a significant difference between children and adults, with children having a larger activation size than adults [$t(123) = 2.40$, $P < 0.05$], but the correlation coefficient failed to reach significance ($r = -0.10$, $P = 0.28$). Activation size correlated significantly with character reading at four ROIs: the left mid-inferior frontal regions (ROI 1, $r = -0.21$, $P < 0.05$), medial frontal cortex and SMA (ROI 2, $r = -0.32$, $P < 0.001$), left caudate nucleus and thalamus (ROI 4, $r = -0.25$, $P < 0.01$), and right inferior frontal cortex and insula (ROI 5, $r = -0.21$, $P < 0.05$).

Development of GM density at the seven ROIs showed nonlinear decreasing patterns similar to those reported by Sowell et al. (2003) (see Fig. 3c). GM density at six ROIs showed significant negative correlations with age and were significantly different between children and adults (two-tailed,

Table 3 Simple and partial correlations between age, character reading, and (i) average BOLD activation (ii) activation cluster size, (iii) GM density, and (iv) WM density in the seven ROIs across all participants

	Simple correlation				Partial correlation controlling for character reading performance		Partial correlation controlling for homophone decision accuracy score		Simple correlation				Partial correlation controlling for age	
	All participants ($n = 125$)		Performance matched ($n = 48$)		All participants ($n = 125$)		All participants ($n = 125$)		All participants ($n = 125$)		Performance matched ($n = 48$)		All participants ($n = 125$)	
	r	P	r	P	r	P	r	P	r	P	r	P	r	P
(i) Between average BOLD activation and														
	Age								Character reading					
ROI 1	**−0.33**	< 0.001	−0.31	= 0.033	**−0.29**	= 0.001	−0.20	= 0.024	**−0.23**	= 0.012	0.02	= 0.881	−0.17	= 0.065
ROI 2	**−0.38**	< 0.001	−0.29	= 0.043	**−0.34**	< 0.001	−0.20	= 0.029	**−0.33**	< 0.001	−0.02	= 0.888	**−0.27**	= 0.003
ROI 3	**−0.24**	= 0.007	−0.15	= 0.321	**−0.21**	= 0.024	−0.07	= 0.460	**−0.19**	= 0.037	−0.05	= 0.715	−0.15	= 0.114
ROI 4	**−0.33**	< 0.001	−0.22	= 0.126	**−0.28**	= 0.002	−0.19	= 0.033	**−0.32**	< 0.001	−0.06	= 0.710	**−0.26**	= 0.004
ROI 5	**−0.43**	< 0.001	−0.33	= 0.023	**−0.41**	< 0.001	−0.23	= 0.009	**−0.22**	= 0.017	0.09	= 0.540	−0.14	= 0.136
ROI 6	0.02	= 0.859	0.07	= 0.620	0.05	= 0.624	0.05	= 0.584	−0.12	= 0.212	0.03	= 0.866	−0.12	= 0.186
ROI 7	**−0.25**	= 0.006	−0.13	= 0.398	**−0.22**	= 0.017	−0.08	= 0.395	**−0.20**	= 0.028	−0.03	= 0.825	−0.15	= 0.097
(ii) Between average activation cluster size and														
	Age								Character reading					
ROI 1	−0.08	= 0.356	−0.03	= 0.849	−0.04	= 0.691	−0.02	= 0.869	**−0.21**	= 0.021	−0.11	= 0.474	−0.20	= 0.031
ROI 2	**−0.25**	= 0.006	−0.16	= 0.281	−0.19	= 0.042	−0.09	= 0.322	**−0.32**	< 0.001	−0.13	= 0.381	**−0.28**	= 0.002
ROI 3	0.11	= 0.209	0.18	= 0.220	0.15	= 0.114	0.17	= 0.064	−0.12	= 0.187	−0.21	= 0.161	−0.15	= 0.100
ROI 4	−0.10	= 0.280	0.10	= 0.516	−0.05	= 0.624	−0.04	= 0.686	**−0.25**	= 0.006	−0.11	= 0.467	**−0.24**	= 0.010
ROI 5	**−0.22**	= 0.013	−0.06	= 0.710	−0.19	= 0.042	−0.05	= 0.608	**−0.21**	= 0.022	−0.06	= 0.683	−0.17	= 0.070
ROI 6	0.14	= 0.108	0.06	= 0.665	0.17	= 0.075	0.09	= 0.302	−0.04	= 0.634	−0.06	= 0.711	−0.08	= 0.387
ROI 7	−0.01	= 0.951	0.20	= 0.185	0.02	= 0.817	0.07	= 0.425	−0.13	= 0.169	−0.12	= 0.403	−0.13	= 0.165
(iii) Between GM density and														
	Age								Character reading					
ROI 1	**−0.79**	< 0.001	**−0.79**	< 0.001	**−0.79**	< 0.001	**−0.70**	< 0.001	**−0.22**	= 0.014	0.24	= 0.107	−0.08	= 0.386
ROI 2	**−0.74**	< 0.001	**−0.71**	< 0.001	**−0.73**	< 0.001	**−0.63**	< 0.001	**−0.21**	= 0.019	0.19	= 0.208	−0.08	= 0.413
ROI 3	**−0.56**	< 0.001	**−0.58**	< 0.001	**−0.55**	< 0.001	**−0.44**	< 0.001	**−0.21**	= 0.025	0.09	= 0.537	−0.10	= 0.289
ROI 4	**−0.34**	< 0.001	−0.24	= 0.098	**−0.29**	= 0.002	−0.12	= 0.184	**−0.39**	< 0.001	−0.18	= 0.225	**−0.34**	< 0.001
ROI 5	**−0.73**	< 0.001	**−0.69**	< 0.001	**−0.72**	< 0.001	**−0.62**	< 0.001	−0.15	= 0.102	0.31	= 0.033	0.02	= 0.862
ROI 6	**−0.75**	< 0.001	**−0.72**	< 0.001	**−0.74**	< 0.001	**−0.62**	< 0.001	**−0.30**	= 0.001	0.07	= 0.636	−0.21	= 0.022
ROI 7	−0.16	= 0.085	−0.03	= 0.861	−0.11	= 0.230	0.01	= 0.875	**−0.24**	= 0.008	−0.17	= 0.252	−0.21	= 0.020
(iv) Between WM density and														
	Age								Character reading					
ROI 1	**0.45**	< 0.001	**0.55**	< 0.001	**0.43**	< 0.001	**0.37**	< 0.001	**0.26**	= 0.004	0.11	= 0.456	0.19	= 0.043
ROI 2	**0.35**	< 0.001	**0.49**	< 0.001	**0.33**	< 0.001	**0.31**	< 0.001	**0.21**	= 0.022	0.09	= 0.565	0.14	= 0.122
ROI 3	**0.22**	= 0.012	0.25	= 0.092	**0.19**	= 0.042	0.16	= 0.085	**0.31**	= 0.001	0.25	= 0.090	**0.27**	= 0.003
ROI 4	**0.49**	< 0.001	**0.61**	< 0.001	**0.48**	< 0.001	**0.38**	< 0.001	**0.33**	< 0.001	0.08	= 0.591	**0.26**	= 0.005
ROI 5	**0.44**	< 0.001	**0.49**	< 0.001	**0.42**	< 0.001	**0.36**	< 0.001	**0.26**	= 0.004	0.19	= 0.206	0.19	= 0.044
ROI 6	0.16	= 0.074	0.25	= 0.088	0.14	= 0.129	0.12	= 0.176	0.14	= 0.124	0.19	= 0.187	0.11	= 0.239
ROI 7	**0.52**	< 0.001	**0.63**	< 0.001	**0.51**	< 0.001	**0.40**	< 0.001	**0.35**	< 0.001	0.14	= 0.342	**0.28**	= 0.002

ROI 1: the left mid-inferior frontal regions. ROI 2: the medial frontal cortex and SMA. ROI 3: the left fusiform gyrus and bilateral striate and extrastriate cortices. ROI 4: the left caudate nucleus and thalamus. ROI 5: the right inferior frontal cortex and insula. ROI 6: the left SPL. ROI 7: the right caudate nucleus and putamen. Correlation coefficients in bold print are statistically significant after Holm–Bonferroni correction at $P < 0.05$.

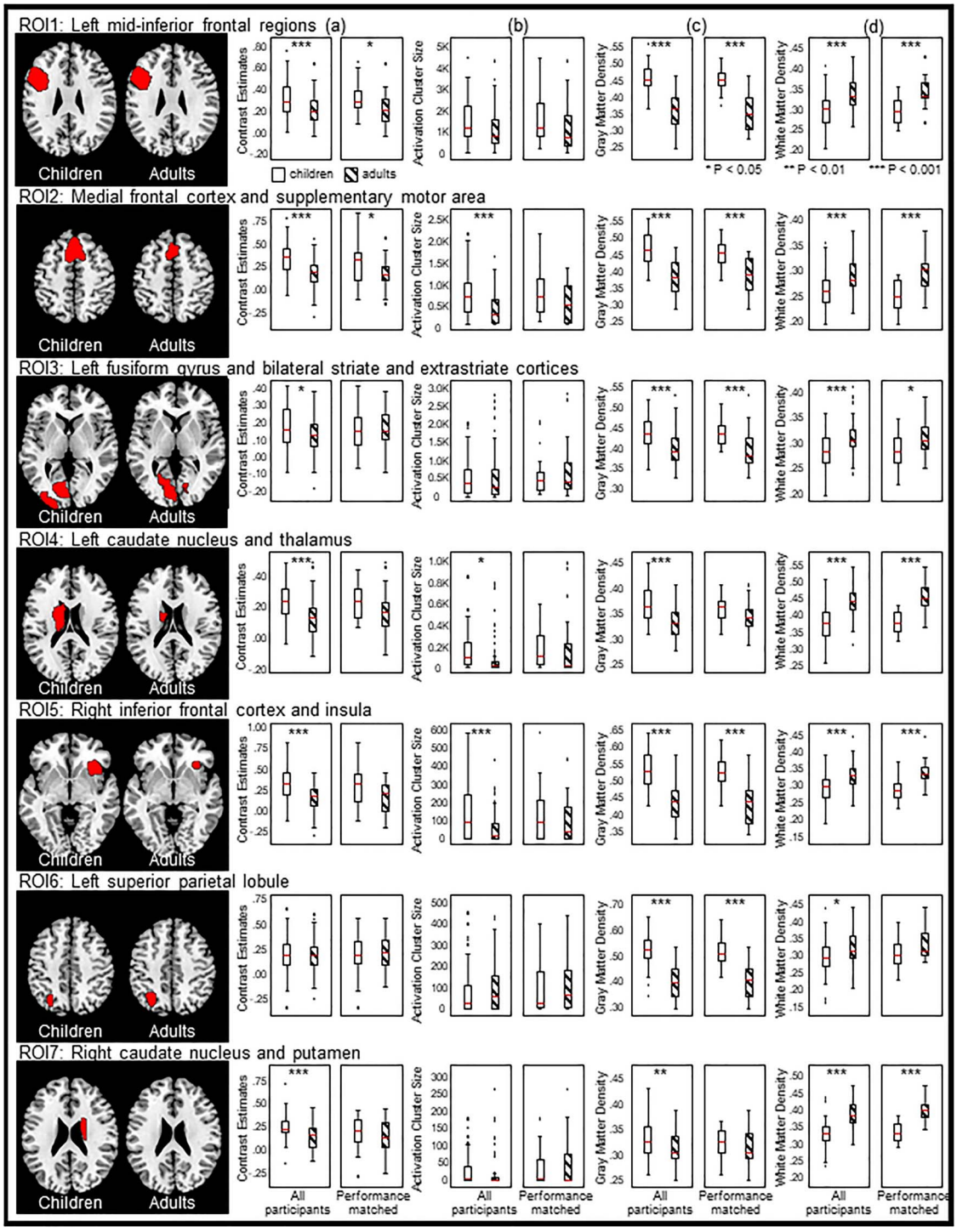

Figure 4. ROI-based independent-samples *t*-tests on four brain measures: (*a*) BOLD activity, (*b*) activation cluster size, (*c*) GM density, and (*d*) WM density between children and adults. Columns (*a*)–(*d*), left panels, across all participants; right panels, the sample matched on character performance and homophone decision accuracy score.

Holm–Bonferroni corrected at $P < 0.05$). These ROIs included the left mid-inferior frontal regions [ROI 1, $r = -0.79$, $P < 0.001$; $t(123) = 11.50$, $P < 0.001$], medial frontal cortex and SMA [ROI 2, $r = -0.74$, $P < 0.001$; $t(123) = 9.68$, $P < 0.001$], left FG and striate–extrastriate cortices [ROI 3, $r = -0.56$, $P < 0.001$; $t(123) = 6.24$, $P < 0.001$], left caudate nucleus and thalamus [ROI 4, $r = -0.34$, $P < 0.001$; $t(123) = 5.80$, $P < 0.001$], right inferior frontal cortex and insula [ROI 5, $r = -0.73$, $P < 0.001$; $t(123) = 9.20$, $P < 0.001$], and left SPL [ROI 6, $r = -0.75$, $P < 0.001$; $t(123) = 12.00$, $P < 0.001$]. Children had a larger GM density in the right caudate nucleus and putamen (ROI 7) than adults [$t(123) = 3.15$, $P < 0.005$], but the correlation coefficient failed to reach significance ($r = -0.16$,

Table 4 Independent-samples *t*-tests between children and adults on (a) BOLD activation, (b) activation cluster size, (c) GM density, and (d) WM density in the seven ROIs across (1) all participants and (2) the character reading and homophone decision accuracy-matched sample

	(a) BOLD activation		(b) Activation cluster size		(c) GM density		(d) WM density	
	t statistics	*P* value	*t* statistics	*P* value	*t* statistics	*P* value	*t* statistics	*P* value
(1) All participants (60 children and 65 adults)								
ROI 1 activation	**3.96**	< 0.001	1.93	= 0.056	**11.50**	< 0.001	**−6.40**	< 0.001
ROI 2	**5.37**	< 0.001	**4.36**	< 0.001	**9.68**	< 0.001	**−5.06**	< 0.001
ROI 3	**2.51**	= 0.013	-0.09	= 0.929	**6.24**	< 0.001	**−3.97**	< 0.001
ROI 4	**4.90**	< 0.001	**2.40**	= 0.018	**5.80**	< 0.001	**−8.03**	< 0.001
ROI 5	**5.25**	< 0.001	**3.53**	= 0.001	**9.20**	< 0.001	**−6.01**	< 0.001
ROI 6	0.04	= 0.971	-0.91	= 0.364	**12.00**	< 0.001	**−2.44**	= 0.016
ROI 7	**3.60**	< 0.001	1.24	= 0.216	**3.15**	= 0.002	**−8.38**	< 0.001
(2) The sample matched on character reading and homophone decision accuracy (24 children and 24 adults)								
ROI 1 activation	2.26	= 0.028	0.82	= 0.417	**7.07**	< 0.001	**−5.06**	< 0.001
ROI 2	2.30	= 0.026	1.79	= 0.080	**5.00**	< 0.001	**−4.94**	< 0.001
ROI 3	0.17	= 0.868	-0.68	= 0.501	**3.66**	< 0.001	**−2.58**	= 0.013
ROI 4	1.70	= 0.097	0.10	= 0.925	1.93	= 0.060	**−6.56**	< 0.001
ROI 5	1.89	= 0.065	0.99	= 0.328	**5.27**	< 0.001	**−4.47**	< 0.001
ROI 6	-0.56	= 0.581	-0.36	= 0.724	**7.08**	< 0.001	-2.00	= 0.052
ROI 7	0.80	= 0.429	-0.46	= 0.645	0.67	= 0.504	**−7.16**	< 0.001

ROI 1: the left mid-inferior frontal regions. ROI 2: the medial frontal cortex and SMA. ROI 3: the left fusiform gyrus and striate–extrastriate cortices. ROI 4: the left caudate nucleus and thalamus. ROI 5: the right inferior frontal cortex and insula. ROI 6: the left SPL. ROI 7: the right caudate nucleus and putamen *t* statistics in bold print are statistically significant after Holm–Bonferroni correction at $P < 0.05$.

$P = 0.09$). GM density also showed small yet significant negative correlations with character reading at six ROIs: the left mid-inferior frontal regions (ROI 1, $r = -0.22$, $P < 0.05$), medial frontal cortex and SMA (ROI 2, $r = -0.21$, $P < 0.05$), left FG and striate–extrastriate cortices (ROI 3, $r = -0.21$, $P < 0.05$), left caudate nucleus and thalamus (ROI 4, $r = -0.39$, $P < 0.001$), left SPL (ROI 6, $r = -0.30$, $P < 0.001$), and right caudate nucleus and putamen (ROI 7, $r = -0.24$, $P < 0.01$).

The WM density correlated positively with age and character reading at six ROIs, including the left mid-inferior frontal regions (ROI 1, $r = 0.45$, $P < 0.001$ for age and $r = 0.26$, $P < 0.005$ for character reading), medial frontal cortex and SMA (ROI 2, $r = 0.35$, $P < 0.001$ for age and $r = 0.21$, $P < 0.05$ for character reading), left FG and striate–extrastriate cortices (ROI 3, $r = 0.22$, $P < 0.05$ for age and $r = 0.31$, $P < 0.001$ for character reading), left caudate nucleus and thalamus (ROI 4, $r = 0.49$, $P < 0.001$ for age and $r = 0.33$, $P < 0.001$ for character reading), right inferior frontal cortex and insula (ROI 5, $r = 0.44$, $P < 0.001$ for age and $r = 0.26$, $P < 0.005$ for character reading), and right caudate nucleus and putamen (ROI 7, $r = 0.52$, $P < 0.001$ for age and $r = 0.35$, $P < 0.001$ for character reading). WM density was significantly different between children and adults in all the seven ROIs, with adults having higher WM density than children (see Table 4).

Functional differences across ages could reflect either maturational changes or performance differences (Schlaggar et al. 2002). Because children generally have a slower response rate and lower performance accuracy than adults, we created one subset of children and adults who were matched on their in-scanner behavioral performance (accuracy in the homophone and font size judgment tasks) as well as out-of-scanner character reading performance to better control for these performance effects (24 children and 24 adults; Table 1). Average BOLD contrast estimates, activation cluster size, and GM and WM density in the seven ROIs were extracted and computed to see whether age differences could still be observed between the two performance-matched subgroups (Fig. 4, Tables 3 and 4). BOLD activation remained moderately correlated with age in the left mid-inferior frontal, medial frontal cortex/SMA, and right inferior frontal cortex and insula (ROI 1, $r = -0.31$, $P = 0.03$; ROI 2, $r = -0.29$, $P = 0.043$; ROI 5, $r = -0.33$, $P = 0.02$) and differed between children and adults in the left mid-inferior frontal and medial frontal cortex/SMA [ROI 1: $t(46) = 2.26$, $P = 0.028$; ROI 2, $t(46) = 2.30$, $P = 0.026$], but these differences did not survive Holm–Bonferroni correction. Brain activity or activation cluster size in other ROIs did not significantly correlate with age and were not different between the two age groups. GM density in five ROIs remained significantly different between children and adults and correlated with age [ROI 1, $t(46) = 7.07$, $P < 0.001$, and $r = -0.79$, $P < 0.001$; ROI 2, $t(46) = 5.00$, $P < 0.001$, and $r = -0.71$, $P < 0.001$; ROI 3, $t(46) = 3.66$, $P = 0.001$, and $r = -0.58$, $P < 0.001$; ROI 5, $t(46) = 5.27$, $P < 0.001$, and $r = -0.69$, $P < 0.001$; ROI 6, $t(46) = 7.08$, $P < 0.001$, and $r = -0.72$, $P < 0.001$]. WM density in all ROIs except the left SPL (ROI 6) remained significantly different between children and adults (ROI 1, $r = 0.55$, $P < 0.001$; ROI 2, $r = 0.49$, $P < 0.001$; ROI 4, $r = 0.61$, $P < 0.001$; ROI 5, $r = 0.49$, $P < 0.001$; ROI 7, $r = 0.63$, $P < 0.001$), but only ROIs 1, 2, 4, 5, and 7 remained significantly correlated with age (Table 3).

BOLD activity and GM density were moderately correlated across all participants in the left mid-inferior frontal regions (ROI 1, $r = 0.34$, $P < 0.001$), medial frontal cortex/SMA (ROI 2, $r = 0.40$, $P < 0.001$), left caudate nucleus and thalamus (ROI 4, $r = 0.27$, $P < 0.005$), and right inferior frontal cortex and insula (ROI 5, $r = 0.36$, $P < 0.001$) but not in the left FG and striate–extrastriate cortices (ROI 3, $r = 0.18$, $P < 0.05$), left SPL (ROI 6, $r = 0.06$, $P = 0.48$), or right caudate nucleus and putamen (ROI 7, $r = 0.16$, $P = 0.07$) (Table 5). When controlling for character reading and in-scanner performance, no correlation remained statistically significant after Holm–Bonferroni correction. Thus, BOLD activation and GM density were generally weakly correlated, even though both showed a decreasing trend (except caudate nucleus and left superior parietal regions) across the human lifespan. In addition, BOLD activity did not correlate

Table 5 Strengths of the endogenous and modulatory connectivity between the four brain regions among the adult group and the children group (in Hz)

		Endogenous connectivity				Modulatory connectivity			
		From				From			
	To	OCC	FUS	SPL	MFG	OCC	FUS	SPL	MFG
Adults	OCC	—	0.04 (0.98)	0.03 (0.95)	—	—	0.04 (0.63)	−0.02 (0.56)	—
	FUS	0.03 (0.96)	—	0.00 (0.58)	0.01 (0.70)	−0.02 (0.55)	—	−0.05 (0.62)	0.10 (0.77)
	SPL	0.01 (0.77)	0.02 (0.86)	—	0.01 (0.74)	0.02 (0.58)	0.23 (0.92)	—	−0.06 (0.69)
	MFG	—	0.02 (0.86)	0.02 (0.80)	—	—	0.19 (0.88)	0.00 (0.50)	—
Children	OCC	—	0.02 (0.82)	0.01 (0.77)	—	—	0.01 (0.52)	−0.01 (0.55)	—
	FUS	0.02 (0.89)	—	0.01 (0.70)	0.03 (0.93)	0.00 (0.51)	—	−0.01 (0.55)	−0.01 (0.54)
	SPL	0.02 (0.80)	0.01 (0.60)	—	0.02 (0.89)	0.03 (0.59)	—	—	−0.01 (0.52)
	MFG	—	0.02 (0.84)	0.01 (0.68)	—	—	−0.05 (0.64)	0.00 (0.38)	—

The number in the parentheses represents the probability value associated with the connectivity parameter. The modulatory connectivity from FUS to SPL is missing in the children group as family 1 won (the ventral pathway–only family).

significantly with WM density in any of the seven ROIs after Holm–Bonferroni correction, across either the whole sample or the performance-matched sample. These results suggest that regional cortical activation is not determined solely by age or biological structure but is a function of the level of skill.

While children and adults used the same brain network to process Chinese text, changes in connections among the specialized brain regions may be observed between the two age groups. We computed effective connectivity between cortical areas traditionally associated with reading Chinese using DCM. Following the findings of Xu et al. (2015), who reported that Chinese visual word recognition engaged a ventral pathway, with information flowing from the occipital cortex (OCC) to the left fusiform gyrus (FUS), then to the left SPL, and, finally, to the left middle frontal gyrus (MFG), we selected these four regions to compute effective connectivity: the left occipital cortex (OCC, $x = -28$, $y = -94$, $z = -4$), left fusiform gyrus (FUS, $x = -44$, $y = -58$, $z = -16$), left superior parietal region (SPL, $x = -28$, $y = -66$, $z = 44$), and left mid-inferior frontal regions (MFG, $x = -44$, $y = 16$, $z = 26$). Time series of the ROIs (sphere of 6 mm) of each subject were extracted by searching for the subject-specific maxima within a sphere of 8 mm centered at the abovementioned coordinates with a mask of the homophone > font size contrast at a liberal threshold of $P < 0.05$ uncorrected (cf., Xu et al. 2015). We were able extract the time series of all four regions from 75 participants (61%), and the DCM analysis was performed for these participants only. To increase the power of analysis, we grouped grade 1 and grade 4 participants together in the child group and grouped all the adults in the adult group. The child group consisted of 15 grade 1 and 26 grade 4 children, while the adult group consisted of 18 younger and 16 older adults.

We aimed to test how visual information is propagated from the occipital cortex (OCC) to a higher-level language processing area (MFG). We assumed that information would first enter the reading network from the OCC and would pass to the MFG from the FUS, either directly or by passing through the SPL. All four regions were interconnected, but there was no direct connection between the OCC and MFG to reduce the model space (Xu et al. 2015). This resulted in five pairs of forward–backward intrinsic connections (Fig. 5A). The models were then generated by either including or excluding the modulatory effects of homophone judgment on each connection, which gave a total of 2^10 = 1024 models. We classified the models into four families according to the presence of modulatory effects on the ventral (FUS to MFG) pathway and the dorsal (FUS to SPL) pathway. Family-level random-effects BMS and Bayesian model averaging on the winning family were then conducted. The evidence of each family is reported as the exceedance probability (xp), which measures the probability that one family is more likely than the other families to simulate the group data. The exceedance probabilities of the families of the models are summarized in Fig. 5B. The endogenous and modulatory connectivity parameters of the two groups are summarized in Table 5. The endogenous connectivity parameters represent context- or task-independent coupling between brain regions, whereas the modularity connectivity parameters represent task-dependent connections (Friston 2011).

Among the child group, the ventral pathway–only family won, with the highest xp of 0.43. The family in the second place was the family with both pathways (xp = 0.29). This result shows that the ventral pathway from the fusiform gyrus to the mid-inferior frontal area is evident among children. In adults, the family with both pathways best modeled the data (xp = 0.68). Both adults and children had a relatively strong forward endogenous connection from the occipital region to the fusiform gyrus, as expected (0.03 and 0.02 Hz, respectively). Adults were found to have a strong connection from the fusiform gyrus (0.04 Hz) and the SPL (0.03 Hz) back to the occipital region. Children were found to possess a backward connection from the middle

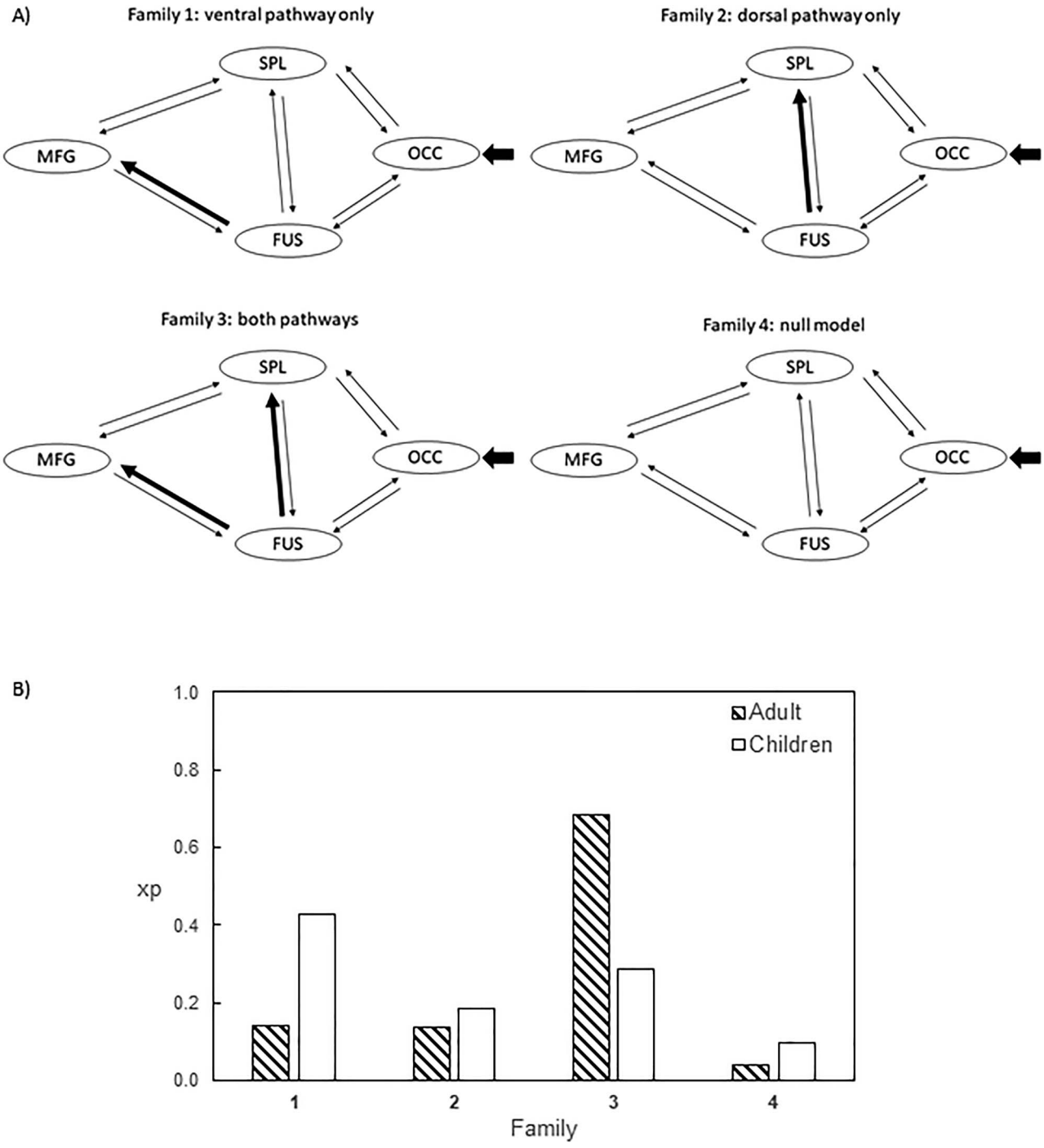

Figure 5. (A) Families of DCM models. The short arrows pointing at OCC represent the input of the effects of the experimental condition (homophone judgment). Thick arrows in families 1–3 represent the presence of the modulatory effects of the experimental condition. Apart from the two connections designated for family partition, all the other connections are allowed to be switched on and off for modulatory effects. This results in $2^8 = 256$ models in each family. (B) The xp of each family in the adult and children group.

frontal region to the fusiform gyrus (0.03 Hz). The positive values of the endogenous parameters indicate that the couplings are excitatory in nature. Strong modulatory effects of homophone judgment were found in the FUS to SPL (0.23 Hz) and FUS to MFG (0.19 Hz) pathways in adults, which showed that reading Chinese enhanced information flow from the fusiform gyrus to both the inferior middle frontal regions and the SPL. Children, in contrast, did not show a clear pattern of modulatory connectivity, given the relatively lower probability values of the parameters. We did not attempt to directly compare the parameters of adults and children because the winning families are different across the two groups.

Discussion

This is the first study to examine the developmental changes in reading-related brain activations across the lifespan. Three key findings have been reported here. First, overlapping neuroanatomical systems were identified in participants of different ages, although differential degrees of activity were observed. This pattern of results is intriguing because it indicates that very early Chinese readers, at age 6–7, already use the same cortical network to recognize visual words as adults. Second, functional activities in the reading-related cortical sites identified in this study were either negatively correlated or were not correlated with age, and age differences diminished when reading performance was matched between the two age groups. In contrast, GM and WM density differed significantly between the two age groups, and GM density correlated negatively with age in most ROIs except the bilateral caudate regions, whereas WM density correlated positively with age in all but the left SPL, regardless of whether reading performance was controlled. These findings suggest that cortical activity is not determined by biological structure, per se, but is also determined by proficiency level in word decoding, with the BOLD activity in the left mid-inferior frontal and medial frontal cortex/SMA being moderately correlated with GM density. Third, connectivity patterns between cortical areas associated with reading were different in children and adults. This finding shows that the neural development of reading is evident in changes in connections among specialized regions, supporting the interactive specialization account.

Consistent with previous findings (Siok et al. 2003, 2004; Tan et al. 2005; Xue et al. 2005; Wu et al. 2012), this study shows that syllable-level reading processing is subserved by a brain network including the left mid-inferior frontal regions (BAs 9/44/45/47); left precentral gyrus (BA 6); right inferior frontal gyrus (BA 47); bilateral insula and superior medial frontal regions (BAs 6/8); dorsal anterior cingulate gyrus (BA 32); left SPL (BA 7); left cuneus (BA 17); left fusiform gyrus (BA 37); bilateral lingual gyrus (BAs 18/19); and subcortical regions such as the caudate nucleus, putamen, thalamus, and cerebellum. Importantly, the left temporoparietal regions, covering the left posterior superior temporal gyrus, angular gyrus, and supramarginal gyrus, which are responsible for phonemic, rule-based analysis and auditory-visual cross-modal mapping processes (Booth et al. 2003; Turkeltaub et al. 2003; Pugh et al. 2005), are not involved in Chinese reading in either beginners or fluent readers. Our findings lend more support to the experience-based theory of cortical regional specialization, which assumes that a specialized region emerges because of the specific tuning of neurons to shape features (e.g., word or character stroke patterns) as a function of skill/experience (Bedny 2018), thus leading to culturally specific reading systems (Coltheart 2004; Siok et al. 2004). The fact that children and adults used the same neural network suggests that brain regions are co-opted to support the computation of features unique to a writing system, and this process starts right at the beginning of reading acquisition. Future studies may also include diffusion tensor imaging to examine the development of structural connectivity of the Chinese reading network and if structural connectivity determines functional connectivity (cf., Carreiras et al. 2009; Saygin et al. 2012, 2016; Srihasam et al. 2014; Osher et al. 2016).

In alphabetic scripts, both regressive (reduced brain activity with age) and progressive (increased brain activity) changes in the neural network for reading have been reported. Regressive changes are mostly found in the right posterior brain regions, including the right inferior temporal sulcus, right precuneus, and right fusiform gyrus (Turkeltaub et al. 2003); the right superior temporal regions (Booth et al. 2002, 2003, 2004); and a few regions in the left hemisphere, such as the left extrastriate cortex (Schlaggar et al. 2002; Brown et al. 2005), left mid-superior temporal cortex, and medial frontal/anterior cingulate gyrus (Brown et al. 2005). Progressive changes, however, have been reported mainly in the left perisylvian language regions, including the left mid-inferior frontal regions (Schlaggar et al. 2002; Gaillard et al. 2003; Turkeltaub et al. 2003; Booth et al. 2004; Brown et al. 2005), left superior frontal gyrus (Turkeltaub et al. 2003; Brown et al. 2005), posterior cingulate gyrus (Turkeltaub et al. 2003; but see Brown et al. 2005, who found regressive change in this region), left middle temporal regions (Turkeltaub et al. 2003), left angular gyrus (Booth et al. 2004), and left supramarginal gyrus (Brown et al. 2005). This pattern of left–progressive, right–regressive change is in line with Orton's lateralization theory of reading development, which postulates that successful reading is contingent upon the disassociation of right visual percepts from the left language regions (Orton 1925; cf. Turkeltaub et al. 2003) and is supported by empirical findings showing that the degree of left lateralization is a positive function of age (e.g., Holland et al. 2001; Brown et al. 2005; Szaflarski et al. 2006; but see Gaillard et al. 2003). This pattern is also in line with the neuronal recycling hypothesis (Dehaene 2009), which postulates that successful reading acquisition relies on accommodation in the perisylvian language regions. This pattern of developmental change, however, is not observed for reading Chinese. The neural network for Chinese reading processing mostly shows regressive changes. One possible interpretation of this difference is that our participants represented a much larger age span while previous studies tested participants aged 6–44 years old. Another possibility is that the pattern of neurodevelopment may be constrained by language and task type. In our study, written Chinese words were employed in a phonology-based judgment task. Chinese characters are read via a memory retrieval process based on "objects" (characters) and their component features, and thus, learning experience practices this rote retrieval and makes it increasingly automatic (Xue et al. 2006; but see Cao et al. 2010). In a phonological task in alphabetic languages, reading is based on the learning of letter–sound conversions and is rule-based. The reading system, thus, heavily relies on the spoken language system.

In conclusion, our findings show that the cortical network for Chinese reading deviates from that used for alphabetic reading, even from the beginning stages of reading acquisition, and this divergent pattern continues throughout the whole lifespan. Our finding that functional activity and gray and WM density are weakly correlated constitutes a challenge to the structural-based hypothesis of the cortical specialization of cognition, which assumes that structure determines function. When skill level, as indexed by performance accuracy, is controlled for, as in this study, there is a weak or no association between brain activity and age. It seems that similar brain regions may be involved in reading in children and adults, but the activity in and connections between these regions are modulated by reading proficiency. Learning experience, instead of pre-existing brain structures, determines reading acquisition. Future research should examine whether and how experience and brain structure interact to determine the development of the cortical regions for reading.

Funding

Shenzhen basic research scheme (JCYJ20170818110103216, JCYJ20170412164413575, 2019SHIBS0003); Guangdong key basic research scheme (2018B030332001); Guangdong Pearl River Talents Plan Innovative and Entrepreneurial Team scheme (2016ZT06S220); National Strategic Basic Research (973) Program of the Ministry of Science and Technology of China (2012CB720701).

Notes

We thank Ping Li for comments on an early version of this manuscript.

References

Bedny M. 2017. Evidence from blindness for a cognitively pluripotent cortex. *Trends in Cogn Sci*. 21:637–648.

Bock DD, Lee WCA, Kerlin AM, Andermann ML, Hood G, Wetzel AW, Yurgenson S, Soucy ER, Kim HS, Reid RC. 2011. Network anatomy and in vivo physiology of visual cortical neurons. *Nature*. 471:177–184.

Booth JR, Burman DD, Meyer JR, Gitelman DR, Parrish TB, Mesulam MM. 2002. Modality independence of word comprehension. *Hum Brain Mapp*. 16:251–261.

Booth JR, Burman DD, Meyer JR, Gitelman DR, Parrish TB, Mesulam MM. 2003. Relation between brain activation and lexical performance. *Hum Brain Mapp*. 19:155–169.

Booth JR, Burman DD, Meyer JR, Gitelman DR, Parrish TB, Mesulam MM. 2004. Development of brain mechanisms for processing orthographic and phonologic representations. *J Cogn Neurosci*. 16:1234–1249.

Briggman KL, Helmstaedter M, Denk W. 2011. Wiring specificity in the direction-selectivity circuit of the retina. *Nature*. 471:183–188.

Brown TT, Lugar HM, Coalson RS, Miezin FM, Petersen SE, Schlaggar BL. 2005. Developmental changes in human cerebral functional organization for word generation. *Cereb Cortex*. 15:275–290.

Burgund ED, Kang HC, Kelly JE, Buckner RL, Snyder AZ, Petersen SE, Schlaggar BL. 2002. The feasibility of a common stereotactic space for children and adults in fMRI studies of development. *Neuroimage*. 17:184–200.

Cao F, Lee R, Shu H, Yang Y, Xu G, Li K, Booth JR. 2010. Cultural constraints on brain development: evidence from a developmental study of visual word processing in mandarin Chinese. *Cereb Cortex*. 20:1223–1233.

Carreiras M, Seghier ML, Baquero S, Estévez A, Lozano A, Devlin JT, Price CJ. 2009. An anatomical signature for literacy. *Nature*. 461:983–986.

Coltheart M. 2004. Brain imaging, connectionism, and cognitive neuropsychology. *Cogn Neuropsychol*. 21:21–25.

Coltheart M. 2014. The neuronal recycling hypothesis for reading and the question of reading universals. *Mind Lang*. 29:255–269.

Courchesne E, Chisum HJ, Townsend J, Cowles A, Covington J, Egaas B, Harwood M, Hinds S, Press GA. 2000. Normal brain development and aging: quantitative analysis at in vivo MR imaging in healthy volunteers. *Radiology*. 216:672–682.

Dehaene S. 2009. *Reading in the brain*. The new science of how we read. New York: Penguin

Dehaene S, Cohen L. 2011. The unique role of the visual word form area in reading. *Trends Cogn Sci*. 15:254–262.

Friston KJ. 2011. Functional and effective connectivity: a review. *Brain Connect*. 1:13–36.

Friston K, Ashburner J, Frith CD, Poline JB, Heather JD, Frackowiak RS. 1995. Spatial registration and normalization of images. *Hum Brain Mapp*. 3:165–189.

Friston KJ, Harrison L, Penny W. 2003. Dynamic causal modelling. *Neuroimage*. 19:1273–1302.

Friston KJ, Price CJ. 2001. Dynamic representations and generative models of brain function. *Brain Res Bull*. 54:275–285.

Gabrieli JDE. 2009. Dyslexia: a new synergy between education and cognitive neuroscience. *Science*. 325:280–283.

Gaillard WD, Balsamo LM, Ibrahim Z, Sachs BC, Xu B. 2003. fMRI identifies regional specialization of neural networks for reading in young children. *Neurology*. 60:94–100.

Giedd JN, Blumenthal J, Jeffries NO, Castellanos FX, Liu H, Zijdenbos A, Paus T, Evans AC, Rapoport JL. 1999. Brain development during childhood and adolescence: a longitudinal MRI study. *Nat Neurosci*. 2:861–863.

Gogtay N, Giedd JN, Lusk L, Hayashi KM, Greenstein D, Vaituzis AC, Nugent TF, Herman DH, Clasen LS, Toga AW *et al*. 2004. Dynamic mapping of human cortical development during childhood through early adulthood. *Proc Natl Acad Sci*. 101:8174–8179.

Golarai G, Ghahremani DG, Whitfield-Gabrieli S, Reiss A, Eberhardt JL, Gabrieli JDE, Grill-Spector K. 2007. Differential development of high-level visual cortex correlates with category-specific recognition memory. *Nat Neurosci*. 10:512–522.

Goswami U, Ziegler JC. 2006. Fluency, phonology and morphology: a response to the commentaries on becoming literate in different languages. *Dev Sci*. 9:451–453.

Holland SK, Plante E, Weber Byars A, Strawsburg RH, Schmithorst VJ, Ball WS. 2001. Normal fMRI brain activation patterns in children performing a verb generation task. *Neuroimage*. 14:837–843.

Johnson MH. 2001. Functional brain development in humans.

Nakamura K, Kuo WJ, Pegado F, Cohen L, Tzeng OJL, Dehaene S. 2012. Universal brain systems for recognizing word shapes and handwriting gestures during reading. *Proc Natl Acad Sci U S A*. 109:20762–20767.

Ofen N, Kao Y-C, Sokol-Hessner P, Kim H, Whitfield-Gabrieli S, Gabrieli JDE. 2007. Development of the declarative memory system in the human brain. *Nat Neurosci*. 10:1198–1205.

Orton ST. 1925. "Word-blindness" in school children. *Arch Neurol Psychiatry*. 14:581.

Osher DE, Saxe RR, Koldewyn K, Gabrieli JDE, Kanwisher N, Saygin ZM. 2016. Structural connectivity fingerprints predict cortical selectivity for multiple visual categories across cortex. *Cereb Cortex*. 26:1668–1683.

Penny WD, Stephan KE, Mechelli A, Friston KJ. 2004. Modelling functional integration: a comparison of structural equation and dynamic causal models. *Neuroimage*. 23:264–274.

Pfefferbaum A, Rohlfing T, Rosenbloom MJ, Chu W, Colrain IM, Sullivan EV. 2013. Variation in longitudinal trajectories of regional brain volumes of healthy men and women (ages 10 to 85 years) measured with atlas-based parcellation of MRI. *Neuroimage*. 65:176–193.

Pugh KR, Sandak R, Frost SJ, Moore D, Mencl WE. 2005. Examining reading development and reading disability in English language learners: potential contributions from functional neuroimaging. *Learn Disabil Res Pract*. 20:24–30.

Rueckl JG, Paz-Alonso PM, Molfese PJ, Kuo W, Bick A, Frost SJ, Hancock R, Wu DH, Mencl WE, Duñabeitia JA *et al*. 2015. Universal brain signature of proficient reading:

evidence from four contrasting languages. *Proc Natl Acad Sci.* 112:15510–15515.

Saygin ZM, Osher DE, Koldewyn K, Reynolds G, Gabrieli JDE, Saxe RR. 2012. Anatomical connectivity patterns predict face selectivity in the fusiform gyrus. *Nat Neurosci.* 15:321–327.

Saygin ZM, Osher DE, Norton ES, Youssoufian DA, Beach SD, Feather J, Gaab N, Gabrieli JDE, Kanwisher N. 2016. Connectivity precedes function in the development of the visual word form area. *Nat Neurosci.* 19:1250–1255.

Schlaggar B, Brown T, Lugar H, Visscher K, Miezin F, Petersen S. 2002. Functional neuroanatomical differences between adults and school-age children in the processing of single words. *Science*. 296:1476–1479.

Siok WT, Jin Z, Fletcher P, Tan LH. 2003. Distinct brain regions associated with syllable and phoneme. *Hum Brain Mapp.* 18:201–207.

Siok WT, Perfetti CA, Jin Z, Tan LH. 2004. Biological abnormality of impaired reading is constrained by culture. *Nature*. 431:71–76.

Snyder PJ, Harris LJ. 1993. Handedness, sex, familial sinistrality effects on spatial tasks. *Cortex*. 29:115–134.

Sowell ER, Peterson BS, Thompson PM, Welcome SE, Henkenius AL, Toga AW. 2003. Mapping cortical change across the human life span. *Nat Neurosci.* 6:309–315.

Srihasam K, Vincent JL, Livingstone MS. 2014. Novel domain formation reveals proto-architecture in inferotemporal cortex. *Nat Neurosci.* 17:1776–1783.

Szaflarski JP, Holland SK, Schmithorst VJ, Byars AW. 2006. fMRI study of language lateralization in children and adults. *Hum Brain Mapp.* 27:202–212.

Talairach J, Tournoux P. 1988. Co-planar stereotaxic atlas of the human brain. 3-dimensional proportional system: an approach to cerebral imaging. NY: Thieme.

Tamnes CK, Herting MM, Goddings A-L, Meuwese R, Blakemore S-J, Dahl RE, Güroğlu B, Raznahan A, Sowell ER, Crone EA *et al.* 2017. Development of the cerebral cortex across adolescence: a multisample study of inter-related longitudinal changes in cortical volume, surface area, and thickness. *J Neurosci.* 37:3402–3412.

Tan LH, Laird AR, Li K, Fox PT. 2005. Neuroanatomical correlates of phonological processing of Chinese characters and alphabetic words: a meta-analysis. *Hum Brain Mapp.* 25: 83–91.

Turkeltaub PE, Gareau L, Flowers DL, Zeffiro TA, Eden GF. 2003. Development of neural mechanisms for reading. *Nat Neurosci.* 6:767–773.

Wu C-Y, Ho M-HR, Chen S-HA. 2012. A meta-analysis of fMRI studies on Chinese orthographic, phonological, and semantic processing. *Neuroimage*. 63:381–391.

Xu M, Wang T, Chen S, Fox PT, Tan LH. 2015. Effective connectivity of brain regions related to visual word recognition: an fMRI study of Chinese reading. *Hum Brain Mapp.* 36: 2580–2591.

Xue G, Chen C, Jin Z, Dong Q. 2006. Cerebral asymmetry in the fusiform areas predicted the efficiency of learning a new writing system. *J Cogn Neurosci.* 18:923–931.

Xue G, Dong Q, Chen K, Jin Z, Chen C, Zeng YW, Reiman ME. 2005. Cerebral asymmetry of children in reading Chinese characters. *Cogn Brain Res*. 24:206–214.